JOURNAL OF EXPERIMENTAL AND THEORETICAL PHYSICS, 2024, Vol. 166, No. 6 (12), pp. 837–846

ELECTRONIC PROPERTIES OF SOLID

# FREQUENCY DEPENDENCE OF VACANCY MOVEMENT HYSTERESIS IN A CLOSED MEMRISTOR BASED ON AN EXACTLY SOLVABLE MODEL OF CONTROLLED NONLINEAR DIFFUSION

© 2024 I. V. Boylo*, K. L. Metlov**

*Galkin Donetsk Institute for Physics and Engineering, Donetsk, 283048 Russia*

** e-mail: boylo@donfti.ru*

*** e-mail: metlov@donfti.ru*

Received August 22, 2024

Revised August 01, 2024

Accepted August 01, 2024

**Abstract**. The frequency dependence of vacancy movement hysteresis in a memristor closed on both sides under the influence of periodic electric current flowing through the memristor is considered. Based on an exactly solvable nonlinear model, an equation for hysteresis loops during the passage of rectangular current pulses with a duty cycle of 2 is obtained. The efficiency of vacancy charge transfer by current compared to their free diffusion is evaluated. It is shown that maximum efficiency is achieved at a specific memristor switching period, which depends on the amplitude of the applied current. Analytical asymptotics of this dependence and memristor resistance depending on the amplitude and period of the current passing through the memristor are obtained.

**DOI:** 10.31857/S004445102412e095

## 1. INTRODUCTION

Memristor, proposed by Leon Chua [1], is a separate type of two-terminal electronic circuit elements whose resistance depends on the time integral of the passed current. If a timedependent current flows through the memristor, its resistance change is accompanied by hysteresis. In other words, the memristor implements a memory function. This simplest analog memory proves to be convenient for implementing electronic synapses in neuromorphic computers [2–10], resistive random-access memory cells [11–13], and electronic devices that allow combining memory and processor [14].

Like the original memristor model [1], most exactly solvable models [12, 15–17] describe memristor evolution using a system of first-order ordinary differential equations in time for several (macroscopic) scalar state variables. When considering spatial variation of state variables (in review [18], such models are proposed to be called distributed), the system of equations is supplemented with partial differential equations (generally nonlinear). Such mesoscopic modeling of memristors is currently performed mainly numerically [19–26].

A significant portion of these approaches can be generalized as a stochastic model with random external force [27, 28], leading to the Fokker-Planck equation for the spatial distribution of defect concentration. In the linear case, this partial differential parabolic equation reduces to the diffusion equation, which allows for fairly accurate description of hysteresis properties of many real devices [18, 27, 28].

Nevertheless, memristors can exhibit strongly nonlinear effects associated, at minimum, with the fact that local defect concentration (mobile vacancies, nuclei of new phase) is limited and cannot exceed certain material-dependent values. This fundamental nonlinearity was investigated by us earlier within a simple mesoscopic model for migration (under applied current) of charged vacancies in a conductor closed on both sides, which reduces to the famous nonlinear Burgers diffusion equation and admits an exact solution [29].

This paper examines a one-dimensional memristor based on a material with mobile charged vacancies,

closed on both sides by flat contacts impermeable to vacancies. Based on the previously obtained exact solution, the hysteresis loops of such memristor are investigated, formed when applying a meander (infinite periodic chain of rectangular pulses with duty cycle 2). The frequency dependence of these loops is calculated and a criterion for determining the optimal switching frequency is proposed.

## 2. MODEL AND EVOLUTION OF VACANCY DISTRIBUTION

Let us consider a material with mobile charged vacancies (although the following consideration is equally applicable to the drift of any other charged defects, including the direct drift of ions) occupying space along the coordinate axis $x$ from $x = 0$ to $x = d$, i.e., a uniform film of thickness $d$ between two flat contacts. We will consider the contacts themselves impermeable to vacancies (chemically inactive). Based on the assumption that the concentration $C$ of mobile vacancies is limited from above by the value $C_{max}$, it is convenient to normalize it to this value: $c = C/C_{max}$, $0 \le c \le 1$. Considering the drift of vacancies under the electric field as a function of time $t$ taking into account the continuity equation, for $c$ we can obtain [29] the Burgers equation

$$\partial_\tau c + p(1-2c)\partial_\xi c = \partial_{\xi\xi} c, \qquad (1)$$

where dimensionless coordinate $\xi = x/d$, time $\tau = tD/d^2$, accounting for the vacancy diffusion coefficient $D$, and parameter $p = \text{const}$, characterizing the strength of external influence, are introduced. In the case when the electric field acting on vacancies with charge $q$ is created by electric current $p_0$ the value $I$, passing through the material with specific resistance

$$p = 2(d/a)\,\mathrm{sh}\left(aq\rho_0 I/k_B\Theta\right)$$

plays the role of renormalized dimensionless current strength. Here, $\Theta$ is the absolute temperature, $k_B$ is the Boltzmann's constant and $a \ll d$ is the characterictic length of a single vacancy jump during drift (to the first order in $a/d$ nothing depends on $a$). The impermeability of boundaries is expressed by the condition [29]

$$pc(1-c) - \partial_\xi c\big|_{x=0,\,d} = 0. \qquad (2)$$

Although both the partial differential equation (1) and the boundary condition (2) are nonlinear, using the Cole-Hopf transformation, one can obtain an exact solution to this boundary value problem [29]

$$c = \frac{\partial}{\partial\xi}\frac{1}{p}\log\left[P + pe^{-\tau p^2/4 + p\xi/2}\sum_{n=1}^{\infty} h_n e^{-\tau n^2\pi^2}\sin n\pi\xi\right], \qquad (3)$$

where

$$P = P(\xi; p, r) = \frac{e^p - e^{pr} - e^{p\xi} + e^{p(r+\xi)}}{e^p - 1},$$

$$r = \int_0^1 c\,d\xi = \text{const}$$

is the total number of mobile vacancies in the system, and coefficients $h_n$ are determined by the initial vacancy distribution $c\,|_{\tau=0} = c_0(\xi)$

$$h_n = 2\int_0^1 \frac{e^{pu_0(\xi)} - P}{p} e^{-p\xi/2}\sin(n\pi\xi)\,d\xi, \qquad (4)$$

where

$$u_0(\xi) = \int_0^\xi c_0(\xi)\,d\xi, \quad u_0(1) = r.$$

On one hand, expressions (3) and (4) allow calculating the evolution of an arbitrary initial vacancy distribution under a given constant external influence (current) $p = \text{const}$. This is sufficient to consider the temporal relaxation of electrical resistance of such a memristor, find its resistance in "on" and "off" states, calculate the write and retention times of information in it [29]. On the other hand, all applications of memristors without exception are based on their hysteresis properties, manifesting under time-dependent external force.

## 3. MEMRISTOR UNDER PERIODIC INFLUENCE

Let's consider the case (often studied in numerical modeling) when the signal applied to the memristor is an infinite periodic (with period $T$) chain of rectangular pulses with a duty cycle of 2. Let's assume that for half the period (duration $T/2$) current $I$, $I > 0$, flows through the memristor, and for the other half – current $-I$. Then the evolution of vacancy distribution can be calculated based on solution (3) with a positive value $p$ in the first half of the period and negative in the second.

The movement of vacancies under the influence of constant current flowing through the memristor during half the period is the relaxation of some initial vacancy distribution to equilibrium (for a given magnitude and polarity of the renormalized current $p$, memristor filling $r$), which is independent of the initial distribution. Mathematically, the relaxation process is expressed in form (3) through the expansion coefficients (4) of the initial vacancy distribution. However, the direction of relaxation and expansion coefficients depend on the current direction (sign $p$). Let's call the values $h_n$ (4) in the first half of the period the expansion coefficients in the forward basis, and in the second half these values, calculated using expression (4) with $p \to -p$, — expansion coefficients in the reverse basis. Then during the influence of current with fixed amplitude, periodically changing sign, the memristor will evolve (relax) half the period in the forward basis, and half in the reverse basis. The final state of the first half-period will be initial for the second half-period. By re-expanding it in the reverse basis, one can calculate the evolution in the second half-period. Then the process repeats.

Infinitely long periodic influence on the memristor leads to periodic evolution of the vacancy distribution (although the finite-time evolution of some initial distribution under such oscillating influence will not immediately reach this cycle). Periodicity means that the coefficients $h_n$ at the beginning of the period can be found from the condition that the vacancy distribution evolved over $T/2$ equals the mirror-reflected relative to $\xi = 1/2$ initial distribution (see Appendix):

$$h_n = \frac{2(-1)^n e^{pr-\frac{p}{2}}}{p} \int_0^1 \left( \overline{P} - \frac{1}{P + pe^{-\frac{p^2(T/2)}{4} + \frac{px}{2}} \sum_{n=1}^{\infty} h_n e^{-n^2\pi^2(T/2)} \sin n\pi\xi} \right) e^{p\xi/2} \sin(n\pi\xi) d\xi, \tag{5}$$

where $\overline{P} = P(\xi; -p, r)$. In the case of an infinitely large period $T \to \infty$ the coefficients $h_n$ correspond to the switching process between equilibrium limit distributions of vacancies, for which there are explicit and analytical expressions (see formula (3.2) from work [29]). But, besides this limit cycle, the dependence of the switching process on frequency is also of interest, and this work is devoted to its analysis.

Unfortunately, in the general case, it is not possible to solve equation (5) analytically. However, this can be done quite effectively numerically, considering that the terms of the sum in the denominator (5) are majorized by a rapidly decaying (at $T > 0$) exponential. Then, truncating at some term (say, under number $k$), we obtain a system of algebraic equations (5) for the first $h_n$, $n = 1,2,\ldots,k$. Using this truncated sum, we can calculate the remaining $h_n$, $n > k$. Moreover, for $T \gg 1$ acceptable accuracy is already given by $k = 1$. For smaller $T$ larger values of $k$, are required, but the calculation still proves to be quite efficient. This algorithm is implemented as a program for Wolfram Mathematica.

Equation (5) can be solved analytically in the limit $pT \ll 1$ for the "optimal" ($r = 1/2$) filling of the memristor, corresponding to the maximum difference of its limit resistances [29]. Then we get

$$h_n = \frac{4(1-(-1)^n)p}{(1+e^{-\frac{T}{8}(p^2+4n^2\pi^2)})n\pi(p^2+4n^2\pi^2)}. \tag{6}$$

The corresponding vacancy distributions are plotted in Fig. 2 below with dotted lines. For small $pT$ they very accurately (visually almost indistinguishably) fall on the solid curves obtained numerically.

Usually, when studying memristor switching under periodic influence, hysteresis loops in current-voltage coordinates are considered ($I$–$V$). For the memristor model discussed here, these loops are schematically shown in the insets to Fig. 1. In coordinates $I$–$V$ they have a typical shape of a rotated figure-eight (in the right inset), and in logarithmic coordinates $I$–$\lg|V|$ they look like seagull wings (in the left inset). Qualitatively similar

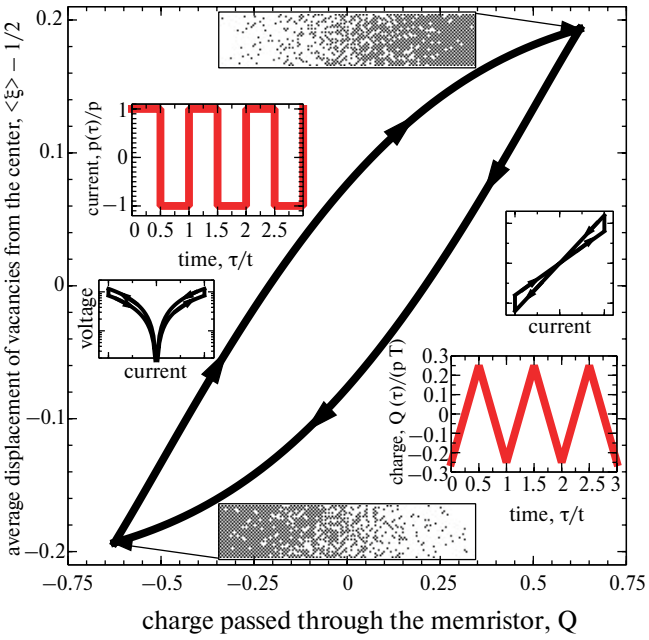


**Fig. 1.** Memristor hysteresis loop (dependence of the average vacancy displacement from the center on the electric charge passed through the memristor $Q$) under periodic external influence for $p = 10$, $T = 0.25$; point clouds show possible realizations of vacancy distribution in two limiting states; insets show normalized dependencies of current $I$ and charge $Q$ on time and (schematically) the same hysteresis loop in current-voltage coordinates ($I$–$V$ and $I$–$\lg|V|$)

loops are observed in many experiments, but such representation of loops is not very convenient for detailed study of memristor hysteresis properties under the influence of a periodic chain of rectangular current pulses. Under such influence on the memristor, the current changes abruptly, and all switching kinetics in coordinates $I$–$V$ is depicted as two vertical lines corresponding to the maximum and minimum current values. Movement along the inclined lines (or seagull wing contours) on the hysteresis loop occurs instantly at the moment of current sign change passing through the memristor. Real memristors always have some capacitance, which causes the current pulses passing through them to be not perfectly rectangular. This leads to rounding of the hysteresis loop corners on the diagram $I$–$V$. Nevertheless, in this work, the memristor capacitance is not taken into account and is considered to be zero.

On the other hand (and this is the central idea behind distinguishing memristors as a separate class of electrical elements [1]), the controlling parameter of the memristor is not the magnitude of the current flowing through it, but the total electrical charge that has passed up to the present moment. An obvious candidate for the role of the state variable is the memristor's resistance, which we will calculate in Section 4. However, the resistance only reflects the distribution of vacancies, which determines the current non-equilibrium state of the memristor. It is also necessary to consider the presence of multiple microscopic mechanisms of memristor resistance formation, which can moreover be engaged simultaneously. These mechanisms are associated with changes in material resistance as a function of local vacancy concentration or with changes in memristor interface resistance when vacancy concentration near them changes. To abstract from resistance formation mechanisms and focus our consideration on the direct cause of the memristor's hysteresis properties, we will choose as the state variable the average displacement of vacancies, which is convenient to measure from the center of the memristor: $\langle\xi\rangle - 1/2$. It is in these coordinates (charge-displacement) that the hysteresis loops are shown in Fig. 1 and Fig. 2.

It is even more convenient to use the dimensionless value of displaced charge

$$\Omega = r(\langle\xi\rangle - 1/2), \tag{7}$$

which is obtained by multiplying the average displacement by the total number of vacancies $r$. Simple displacement for $r < 1/2$ is always greater than displacement for $r > 1/2$, since in the second case, a significant number of vacancies do not move, which reduces the average displacement value. The value $\Omega$ is extensive and therefore corresponds to the expected symmetry between memristors with filling numbers $r$ and $1 - r$. Expected because, generally speaking, the processes of displacement of vacancies and impurity atoms (whose absence constitutes a vacancy) have the same kinetics with only the minor difference that vacancies and impurity atoms have charges of opposite signs and move under the action of the same current in the opposite directions. The presence of this symmetry is visible in the inset to Fig. 3, where the hysteresis curves for $r = \gamma$ and $r = 1 - \gamma$ coincide for all $0 < \gamma < 1$. The charge displacement for $r = 1/2$ is maximal in this case.

The memristor operates in two modes: vacancy displacement by electric current (information writing) and their free diffusion (information storage). To evaluate the efficiency of charge displacement during the writing process, it can be compared

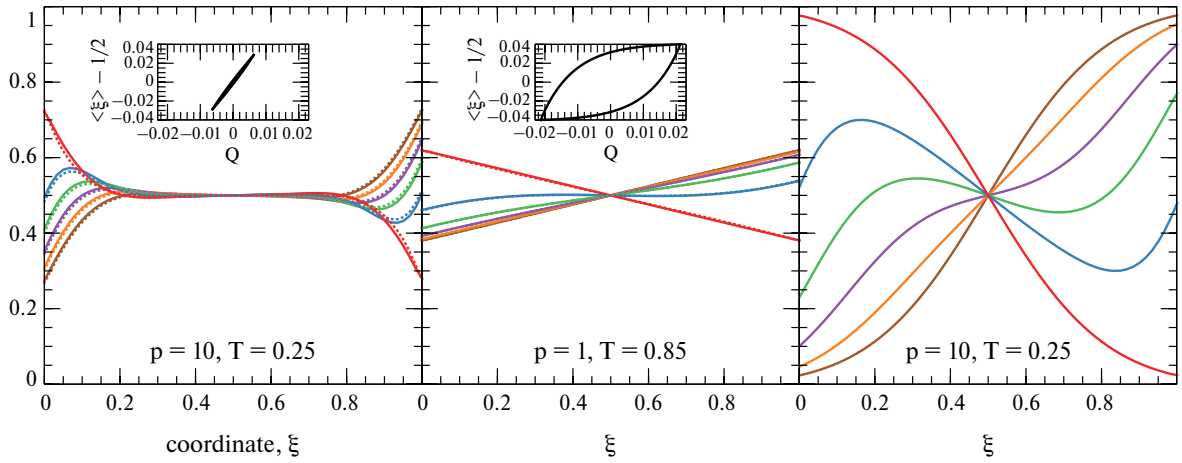


**Fig. 2.** Characteristic distributions of vacancies at $t = 0, T/10, 2T/10, 3T/10, 4T/10, T/2$ (top to bottom along the left side of the graph, or bottom to top along the right) and hysteresis loops (in the insets) for $r = 1/2$ and different values of $p$ and $T$, shown on the graphs. The loop for $p = 10$ and $T = 0.25$ is shown in Fig. 1

with the average displacement of vacancies during free diffusion over the same characteristic time $T$. The latter in the considered one-dimensional case (and in the used normalization) equals $\sqrt{2T}$. The displacement $\Omega$, as defined by formula (7), corresponds to a quarter of the period. Therefore, the sought value characterizing the relative charge displacement equals $4\Omega/\sqrt{2T}$. Its dependence on the switching period $T$ at $r = 1/2$ is plotted in Fig. 3.

The dependence in Fig. 3 for all $p > 0$ contains a maximum. For small periods, the current does not have time to affect the vacancy distribution, and for large periods, the vacancy distribution under current influence reaches a steady state, and further exposure does not increase the lifetime of the recorded information. The position of the maximum $T_{max}$ shifts towards smaller periods with an increase in the normalized current strength $p$. Its magnitude grows accordingly. This means that increasing the memristor's operating speed, to maintain its peak efficiency, also requires an increase in the recording current strength. The presence of a maximum in the frequency dependence of the normalized charge, associated with the "confrontation" between thermal fluctuations erasing information and periodic current pulses recording it, may suggest a similarity between this effect and the recently discovered phenomenon of stochastic resonance in memristors [30]. However, it should be noted that in our case, the numerator and denominator of the ratio $4\Omega/\sqrt{2T}$, generally speaking, refer to different experiments with different time dependencies of the current passing through the memristor: in one of them, information is cyclically recorded, in the second, it is spontaneously erased under the influence of thermal fluctuations in the absence of current. These two processes (information recording and storage) are fundamental in the operation of memristorbased memory cells.

For the value of the switching period $T_{max}$, corresponding to the highest efficiency, two analytical estimates can be made, shown in Fig. 3 by dotted lines. First, this value is bounded from above by $T_{max} < \sqrt{17/90}$, which provides a fairly accurate estimate for $T_{max}$ at $p \ll 1$. The existence of this finite limit is associated with the fact that the motion of vacancies at small $p$ approaches free diffusion. On the other hand, at large $p \gg 1$ asymptotically $T_{max} \simeq 2\sqrt{2}/p$. Since the main properties of memristors manifest themselves precisely at high recording currents $I$, the latter estimate establishes a relationship between the recording current strength in a memristor with free vacancies and its characteristic switching time. In dimensional units (seconds) in the limit $a \to 0$ this time equals

$$\tau_{max} = \sqrt{2} dk_B \Theta / DIq\rho_0.$$

It follows that reducing the memristor thickness also allows increasing the switching speed while maintaining relative efficiency. However, it should be noted that the absolute value of the retention time of written information, which grows quadratically at high currents as a function of $d$ [29], is just as important as the relative efficiency of their

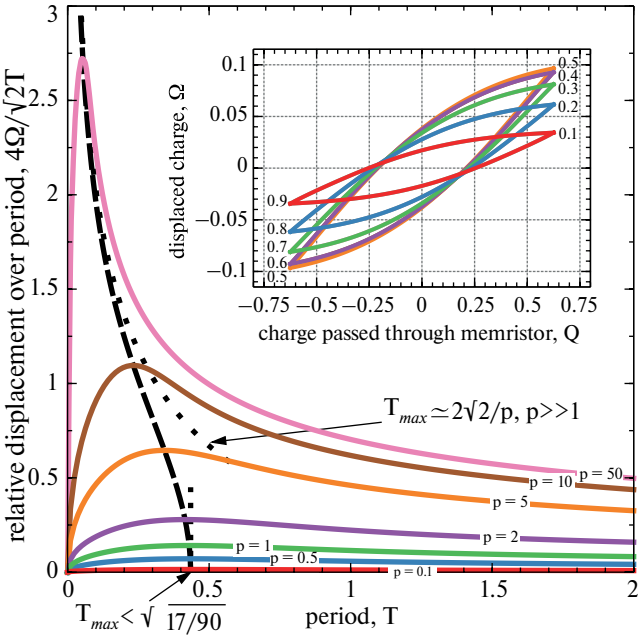


**Fig. 3.** The average displacement of vacancies over the period $T$ normalized to the square root of mean square displacement under simple diffusion, for different $T$, $p$ and $r = 1/2$, the dashed line shows the position of the maximum in this dependence, dotted lines show the asymptotics to the dashed line; the inset shows the dependence of hysteresis loops at $p = 10$, $T = 0.25$ on the duty cycle $r$, where the vertical coordinate is proportional to the total charge displaced by vacancies $\Omega$

displacement. Both these analytical asymptotics may prove useful in designing memristors with predetermined properties.

The above expression for $\tau_{max}$ contains material parameters that are not always precisely known a priori. It is possible to obtain an expression more convenient for comparison with experiment in terms of directly measurable quantities. To do this, we note that the evolution of the memristor state is a relaxation process. Moreover, from very general thermodynamic considerations, it is known that relaxation from a state close to equilibrium usually follows an exponential law. Thus, when approaching the limit state, the memristor resistance depends on time as

$$R(\tau) \propto e^{-\tau/\tau_R},$$

which for our model is directly confirmed by direct calculation [29]. In the same work, an analytical expression for the relaxation time was obtained, which does not depend on the filling coefficient $r$ or the initial distribution of vacancies in the memristor and in the limit $a \to 0$ has the following form

$$\tau_R \approx \frac{d^2}{4D(\pi^2 + (dq\rho_0 I)^2/(k_B\Theta)^2)}.$$

In its physical meaning, this value determines the characteristic information writing time dependent on the external current magnitude $\tau_W = \tau_R$. And this same value, if we set $I = 0$, in it, gives the characteristic time of spontaneous erasure of recorded information when no current flows through the memristor:

$$\tau_E = \tau_R|_{I=0} = \frac{d^2}{4\pi^2 D}.$$

It should be noted that different definitions can be introduced for these characteristic times, which will differ by a methodological (depending on the method) numerical factor; in our further analysis, we will use the above definitions characterizing the memristor relaxation as it approaches its final equilibrium state. In any case, these characteristic times are directly measurable quantities in the experiment. Considering $\tau_W$ and $\tau_E$ known, we can exclude all other parameters from the above expression for $\tau_{max}$:

$$\tau_{max} = \frac{4\sqrt{2}\pi\tau_E}{\sqrt{\tau_E/\tau_W - 1}} \approx 4\sqrt{2}\pi\sqrt{\tau_E\tau_W}. \qquad (8)$$

Moreover, from the definition of $\tau_E$ it follows that always $\tau_W < \tau_E$ and the expression under the root is positive, and the last approximate equality corresponds to the approximation $\tau_W \ll \tau_E$ or (most interesting for applications) the case of large currents $p \gg 1$. The numerical factor in this expression depends on the methodology for determining characteristic times, and it may be different for other definitions.

In other words, we can say that the most effective switching of the memristor is achieved when its switching period equals (with some constant numerical coefficient) the geometric mean of the characteristic write and erase times of information in it. At much longer periods, the current passing through the memristor practically no longer moves vacancies, and therefore does not change the state of the memristor, i.e., leads to nothing but ohmic losses. At much shorter periods, the memristor's state does not have time to change sufficiently to reliably store the recorded information.

## 4. MEMRISTOR RESISTANCE

Microscopically, the state of the memristor in the considered model is determined by the current concentration of mobile vacancies, $c(\xi,\tau)$. Macroscopically, a convenient state variable is the vacancy charge displacement $\Omega$, which directly characterizes the deviation of the vacancy distribution from equilibrium with $\Omega = 0$. The change in $\Omega$ depending on the total electron charge passed through the memristor (being the control parameter of the memristor [1]) is discussed in the previous section.

On the other hand, the value $\Omega$ is not always available for direct measurements. Usually, instead of it, the experiment records the total resistance of the memristor, which we will now calculate. Let us recall that in our work, we consider memristors with contacts impermeable to vacancies. The total number of vacancies inside the memristor thus remains constant. This type of memristors seems to us the most practically important. Although in the case of open (for example, from one side) memristors, it is possible to achieve a greater amplitude of resistance change per cycle, such devices may be sensitive to the characteristics of their external environment (for example, to the oxygen concentration in it, if the memristors are based on oxygen vacancy movement). Beyond our analytical consideration will remain multilayer memristors, in which some layers can act as vacancy accumulators. They also allow consideration based on equations (for each layer) of nonlinear diffusion, but their analytical solution will be much more cumbersome with many additional parameters.

Let us take a phenomenological approach and assume that the specific resistance of the material $p$ (weakly) depends on the concentration of mobile vacancies $c$. Let us represent this dependence in the form of a power series:

$$\rho = \rho_0' + \rho_1 c + \rho_2 c^2 + \dots$$

Since the total number of vacancies inside the memristor does not change, the first-order term only contributes a constant value to the total resistance of the memristor and can be combined with the zero-order term $\rho_0 = \rho_0' + \rho_1 r$. Higher-order terms can lead to resistance changes during vacancy redistribution, but mirror-symmetric distributions (relative to the memristor center) occurring at the limit points of its cycle (when vacancies concentrate near either contact) will correspond to the same total resistance value. This means that even if the dependence of material's specific resistance on vacancy concentration affects memristor operation, it does not impact the resistance difference between the memristor's "on" and "off" states.

Thus, in the first order of , the total resistance of the closed memristor will depend only on the contribution of its interfaces [29]:

$$\rho = \rho_0 + \frac{\kappa_{1,0} + \kappa_{1,1} c}{d}\delta(\xi) + \\ + \frac{\kappa_{2,0} + \kappa_{2,1} c}{d}\delta(\xi - 1) + O(c^2), \quad (9)$$

where $\kappa_{i,0}$ and $\kappa_{i,1}$ — are the expansion coefficients of the surface resistance of interfaces $i = 1,2$ in powers of $c$, and the Dirac delta function $\delta(x)$ is assumed to be left-sided (this mathematical technique formally places it outside the vacancy movement region). Then in the first order, the memristor resistance has the form

$$R = R_0' + R_1 c(0,\tau) + R_2 c(1,\tau),$$

where

$$R_0' = (d\rho_0 + \kappa_{1,0} + \kappa_{2,0})/A,$$

$$R_1 = \kappa_{1,1}/A, \quad R_2 = \kappa_{2,1}/A,$$

$A$ is the contact surface area (memristor cross-section). By regrouping terms, the resistance can be expressed through the dimensionless parameter $\sigma'$ as

$$R = R_0 + R_1\sigma'$$

$$\sigma' = c(0,\tau) + \alpha c(1,\tau) - r(1+\alpha) \quad (10)$$

$$R_0 = R_0' + R_1 r(1+\alpha),$$

where a dimensionless coefficient of interface resistance asymmetry $\alpha = R_2/R_1$ is introduced. The convenience is that the value $\sigma'$ during memristor switching changes symmetrically relative to the point $Q = 0$, $\sigma' = 0$. The value $R_0$ sets the constant component of resistance, while $R_1$ is proportional to the absolute amplitude of its changes.

Further, we will consider the most interesting case of half-filling $r = 1/2$ of the memristor, when the displacement of vacancy charge and change in memristor resistance [29] are maximal. Then the identity $c(1,\tau) = 1 - c(0,\tau)$ holds, which

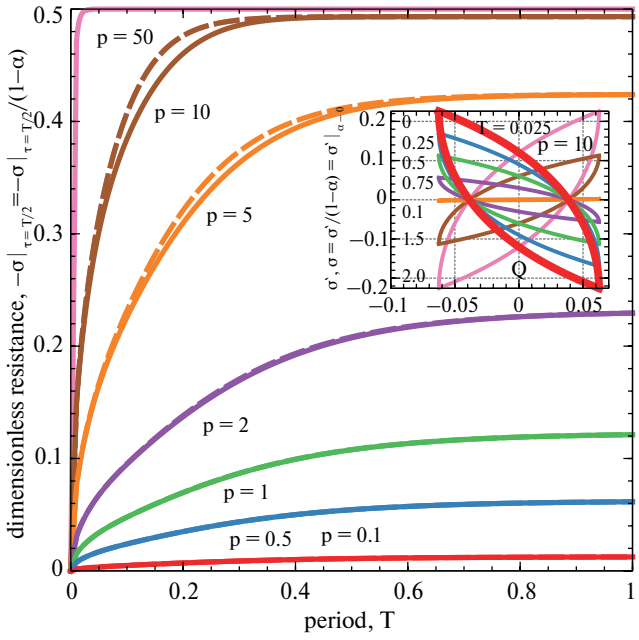


**Fig. 4.** The amplitude of resistance change $-\sigma|_{\tau=T/2}$ during the switching process of a memristor with half ($r = 1/2$) filling: solid lines – exact calculation, dashed lines – asymptotics (12); the inset shows resistance hysteresis loops σ′, depending on the contact asymmetry coefficient α (its values for each loop are labeled with numbers on the left), and the limiting loop (thicker line) $\sigma = \sigma'|_{\alpha=0}$

allows excluding parameter α, considering the renormalized dimensionless resistance of the memristor at $r = 1/2$:

$$\sigma = \sigma'/(1-\alpha) = c(0,\tau) - 1/2 = \sigma'\big|_{\alpha=0}. \quad (11)$$

The inset to Fig. 4 shows hysteresis loops in coordinates $\sigma'$–$Q$ for different values of α, which after renormalization in coordinates σ–$Q$ transform into a universal loop (11), independent of α. A similar rescaling of resistance relaxation curves into a universal curve was obtained in work [31] based on the VEOVM model [20] and experimentally confirmed there (see Fig. 4 in work [31]) for a memristor based on polycrystalline $La_{0.325}Pr_{0.300}Ca_{0.375}MnO_3$ (LPCMO) with silver contacts. It apparently is a universal property of both open and closed on both sides memristors.

When the interfaces are absolutely identical ($\alpha = 1$), there is no change in the resistance of the closed memristor (with half-filling) and $\sigma' = 0$, but in the limit $\alpha \to 1$ the renormalized loop in coordinates σ–$Q$ still remains unchanged. This is despite the fact that the overall slope of the loop when transitioning from $\alpha < 1$ to $\alpha > 1$ changes to the opposite, which corresponds to a change in the sign of $\sigma'$.

The amplitude of the resistance hysteresis loop $\sigma|_{\tau=T/2}$ can be calculated directly using formulas (3), (10), (11). However, an approximate explicit expression can also be obtained based on the asymptotics (6) at $r = 1/2$:

$$\sigma\big|_{\tau=T/2} \simeq -4p\sum_{k=0}^{\infty}\frac{\left(\frac{T}{16}\left(p^2+4\pi^2(2k+1)\right)\right)}{p^2+4\pi^2(2k+1)}. \quad (12)$$

This expression correctly reproduces the resistance amplitude both in loops with small period $T \ll 1$, and in loops with large $T \gg 1$, when the resistance reaches saturation:

$$\sigma|_{\tau=T/2,T\gg1} \simeq -(1/2)(p/4).$$

Noticeable error appears only at intermediate values of $p$ and $T$. The loop amplitude and its asymptotics (12) are plotted in Fig. 4 as a function of the oscillation period of the current passing through the memristor for different values of $p$.

The phenomenological description of memristor resistance given above does not directly depend on the specific material and specific mechanism of electrical resistance formation at the contacts. Its main assumption is the possibility to represent the specific resistance (surface or volume) as a power series in $c$, from which, taking into account the conservation of vacancy quantity in the memristor closed on both sides, in the lowest order in powers of expression (10) is obtained. The parameters $R_0$, $R_1$ and α included in it describe the properties of the memristor material and the mechanism of electrical resistance formation at its (asymmetric) contacts. These parameters can be determined from independent measurements or by fitting.

In the case of $R_0 \gg R_1$ the influence of changes in electrical resistance associated with ion redistribution on the electric field driving these ions can be neglected. A simple way to account for this effect without significantly complicating the model is to use the definition

$$p = 2(d/a)sh(aq\rho I/k_B\Theta)$$

as a self-consistency equation by substituting the value $\rho = \rho_0 + \rho_1\sigma'$, which will already depend on the memristor's state. One can expect this to

lead to additional skewing of the hysteresis loops, but detailed investigation of this effect remained beyond the scope of this work. We also did not account for the memristor's capacitance and assumed that the current pulses were perfectly rectangular. Nevertheless, we accurately accounted for nonlinear hysteresis effects associated with the limited concentration of mobile vacancies, which can manifest themselves in various specific implementations of memristors closed on both sides based on different materials and with different types of contacts.

## 5. CONCLUSIONS

We examined the evolution of an exactly solvable nonlinear model of a memristor with mobile charged vacancies under the influence of periodic external current (consisting of rectangular pulses with duty cycle 2). An equation for hysteresis loops was obtained and solved (generally numerically). In the particular case when the amplitude and period of external current oscillations are small, an analytical asymptotic solution of this equation is provided. It is shown that the highest efficiency of vacancy charge transfer is achieved when the memristor is filled with vacancies exactly half of the maximum possible amount. A measure of vacancy transfer efficiency compared to their free diffusion process was introduced and its dependence on the external current period was investigated. This dependence contains a maximum corresponding to the highest ratio of forced vacancy charge displacement over its free diffusion during the same time period. Analytical asymptotics of the external current period corresponding to maximum efficiency were obtained for small and large amplitudes, as well as the asymptotics of resistance hysteresis loop amplitude. For large external current amplitude, the optimal memristor switching period is related to the write time and information storage time by a simple relation (8).

## APPENDIX. MIRROR-SYMMETRIC DISTRIBUTION OF VACANCIES

Evolution of vacancy distribution under the influence of a periodic sequence with period $T$ and duty cycle 2 of alternating rectangular pulses of external current leads to vacancy distributions at times $t$ and $t + T/2$ (with a shift of half a period) being mirror-symmetric relative to point $\xi = 1/2$. Two such distributions, $c(\xi)$ and $\tilde{c}(\xi)$, are related by the equation $c(\xi) = \tilde{c}(1-\xi)$, and their corresponding antiderivative functions $u(\xi) = r - \tilde{u}(1-\xi)$, where $\tilde{c}(\xi) = \tilde{u}'(\xi)$, $\tilde{u}(0) = 0$, $\tilde{u}(1) = r$. By definition (4), the expansion coefficients $u(\xi)$ are equal to

$$u_n = \frac{2}{p}\int_0^1 \left(e^{p(r-\tilde{u}(1-\xi))} - P(\xi;p,r)\right)e^{-p\xi/2}\sin(n\pi\xi)d\xi. \tag{13}$$

After variable substitution $y = 1 - \xi$, using identities $P(1-\xi;p,r) = e^{pr}P(\xi;-p,r)$ and $\sin n\pi(1-y) = (-1)^n \sin n\pi y$ we obtain the relationship between expansion coefficients of mirror-symmetric functions:

$$u_n = e^{pr-p/2}(-1)^n\left(\tilde{u}_n\Big|_{p\to -p}\right). \tag{14}$$

In other words, the expansion coefficients of the vacancy distribution are directly proportional to the expansion coefficients of their mirror-symmetric distribution in the reverse ($p \to -p$) basis. Expression (5) directly follows from this relationship.

## REFERENCES


1. L. Chua, IEEE Trans. Circuit Theory **18**, 507 (1971).
2. M. Prezioso, F. Merrikh-Bayat, B. D. Hoskins et al., Nature **521**, 61 (2015).
3. M. Prezioso, F. Merrikh-Bayat, B. D. Hoskins et al., Sci. Rep. **6**, 21331 (2016).
4. R. Berdan, E. Vasilaki, A. Khiat et al., Sci. Rep. **6**, 18639 (2016).
5. V. Saxena, X. Wu, and K. Zhu, in *Proc. IEEE International Symposium on Circuits and Systems*, ISCAS 2018, 27-30 May 2018, Florence, Italy, DOI: 10.1109/ISCAS.2018.8351766.
6. F. Liu and C. Liu, in *2018 55th ACM/ESDA/IEEE Design Automation Conference (DAC)*, DOI: 10.1109/dac.2018.8465849.
7. T. Ahmed, S. Walia, E. L. H. Mayes et al., Sci. Rep. **9**, 15404 (2019).
8. S. Deswal, A. Kumar, and A. Kumar, AIP Adv. **9**, 095022 (2019).
9. G. Yuan, X. Ma, C. Ding et al., in *2019 IEEE/ACM International Symposium on Low Power Electronics and Design (ISLPED)*, DOI: 10.1109/islped.2019.8824944.
10. N. Wu, A. Vincent, D. Strukov et al., *Memristor hardware-friendly reinforcement learning*, arXiv:cs.ET/2001.06930.

**11.** R. Waser and A. Masakazu, Nat. Mater. **6**, 833 (2007).

**12.** D. B. Strukov, G. S. Snider, D. R. Stewart et al., Nature **453**, 80 (2008).

**13.** A. Sawa, Mater. Today **11**, 28 (2008).

**14.** D. Ielmini and H. S. P. Wong, Nat. Electron. **1**, 333 (2018).

**15.** L. Chua and S. M. Kang, Proc. IEEE **64**, 209 (1976).

**16.** Y. N. Joglekar and S. J. Wolf, Eur. J. Phys. **30**, 661 (2009).

**17.** E. Linn, A. Siemon, R. Waser et al., IEEE Trans. Circuits Syst. I **61**, 2402 (2014).

**18.** J. B. Roldán, E. Miranda, D. Maldonado et al., Adv. Intell. Syst. **5**, 2200338 (2023).

**19.** D. B. Strukov and R. S. Williams, Appl. Phys. A **94**, 515 (2009).

**20.** M. J. Rozenberg, M. J. Sánchez, R. Weht et al., Phys. Rev. B **81**, 115101 (2010).

**21.** N. Ghenzi, M. J. Sánchez, F. Gomez-Marlasca et al., J. Appl. Phys. **107**, 093719 (2010).

**22.** S. Larentis, F. Nardi, S. Balatti et al., IEEE Trans. Electron Devices **59**, 2468 (2012).

**23.** S. Kim, S. Choi, and W. Lu, ACS Nano 8, 2369 (2014).

**24.** A. Marchewka, R. Waser, and S. Menzel, in *2016 International Conference on Simulation of Semiconductor Processes and Devices (SISPAD)*, p. 145, DOI:10.1109/sispad.2016.7605168.

**25.** A. Marchewka, B. Roesgen, K. Skaja et al., Adv. Electron. Mater. **2**, 1500233 (2016).

**26.** I. V. Boylo, Phys. Stat. Sol. (b) **254**, 1600698 (2017).

**27.** N. V. Agudov, A. V. Safonov, A. V. Krichigin et al., J. Stat. Mech. **2020**, 024003 (2020).

**28.** N. Agudov, A. Dubkov, A. Safonov et al., Chaos Solitons Fractals **150**, 111131 (2021).

**29.** I. V. Boylo and K. L. Metlov, Roy. Soc. Open Sci. **8**, 210677 (2021).

**30.** A. Mikhaylov, D. Guseinov, A. Belov et al., Chaos Solitons Fractals **144**, 110723 (2021).

**31.** S. Tang, F. Tesler, F. G. Marlasca et al., Phys. Rev. X **6**, 011028 (2016)